18TH WORLD CONFERENCE ON EARTHQUAKE ENGINEERING
WCEE2024
MILAN

MILAN, ITALY
30TH JUNE - 5TH JULY 2024
www.wcee2024.it

EFFECTIVE STIFFNESS OF NON-RECTANGULAR REINFORCED CONCRETE WALLS FOR SEISMIC DESIGN AND ASSESSMENT

J. Pacheco de Almeida[1], R. Hoult[2], B. Payen[2] & A.A. Correia[3]

[1] Institute of Mechanics, Materials and Civil Engineering, UCLouvain, Belgium, joao.almeida@uclouvain.be

[2] Institute of Mechanics, Materials and Civil Engineering, UCLouvain, Belgium

[3] National Laboratory for Civil Engineering (LNEC), Lisbon, Portugal

Abstract: *The familiar force-based (FB) method of seismic design and analysis of structures is employed worldwide. However, a growing number of codes and standards, including the next-generation Eurocode 8, now include alternative and more accurate displacement-based (DB) approaches. Recent studies have shown that an unsatisfactory determination of the effective stiffness of vertical members is at the heart of significant discrepancies between FB and DB formulations. Therefore, in order to harmonise them, and more generally to enhance the quality of the FB approach, it becomes essential to improve the estimation of the effective stiffness. The latter is estimated, for structural reinforced concrete walls in most design codes, via proposed reduction factors applied to the uncracked wall stiffness. Such reduction factors were based on studies for rectangular cross-section walls, although many walls are in reality non-rectangular. Using the experimental results of a series of walls with different cross-section shapes, the present investigation shows that the reduction factors proposed by design codes are not applicable to non-rectangular cross-section walls, and assesses the ability of nonlinear beam-truss models to determine the effective stiffness according to different procedures to estimate the effective stiffness ratio.*

1 Introduction

The current availability of advanced numerical models – accessible to engineering practice both in terms of complexity and compatibility with project timelines, for the simulation of the nonlinear seismic response of structures, allows for increasingly accurate estimates of the displacement demand in their members. This observation, together with the foreseeable duplication of the number of buildings worldwide over the next 40 years, is pushing building codes to include and regulate the more accurate "displacement-based (DB) approaches" in building design and assessment, to the detriment of the classic and more familiar "force-based (FB) approach". This is, for instance, one of the key changes included in the next generation of Eurocode 8 (prEN 1998–1–1:2022) (CEN, 2022) with respect to the current generation (EN 1998–1:2004) (CEN, 2004), which is under development for expected release around the middle of the present decade. DB verifications rely on a realistic determination of the effective stiffness of structures. In fact, recent studies (Almeida *et al.*, 2022) have shown that an unsatisfactory determination of the effective stiffness of vertical members is at the source of discrepancies between FB and DB approaches. Although DB approaches, as considered by the codes, can in general be based on nonlinear static or dynamic analyses, the effective stiffness is, per definition, obtained from pushover analyses, which the present study will address.

Most medium-to-high-rise buildings worldwide are reinforced concrete (RC) structures; they generally use structural walls as lateral load resisting system, which dominantly control the overall seismic (and wind) response. Per building, RC walls can be very few, and assume different cross-sectional shapes. In this context, the determination of the effective stiffness of RC walls is fundamental as they govern the effective stiffness of the entire structural system. This study addresses solely the effective stiffness of non-rectangular walls along both planar directions, and its objective is multi-fold: (i) to assemble a database of experimental tests and determine, from those tests, the corresponding effective stiffness; (ii) to simulate these same walls with an advanced model available in engineering practice, followed by new determination of the corresponding effective stiffnesses; (iii) to compare critically the results obtained in (i), (ii), and the existing proposals for effective stiffness provided by international design codes. This covers an important gap in the literature; for instance, in the study by Kolozvari *et al.* (2018), wall effective stiffnesses were computed through several approaches, but it focused on rectangular sections. Unfortunately, building core walls are non-rectangular (e.g., U-shaped, H-shaped, E-shaped), and other structural walls also take alternative non-planar geometries (e.g., L-shaped). The variety of non-rectangular wall geometries was also apparent from damage observations of RC buildings after the destructive Turkish earthquake of February 6 2023 (Vuran *et al.*, 2024). Some recent contributions to the effective stiffness of non-rectangular cross-sections start joining the literature, for instance the study by Samanta and Dasgupta (2024), which among other conclusions show that for a specific T-shaped wall the effective stiffness largely depends on the cross-section shape and the yield strength of the rebars.

With regards to simulation, the Eurocode 8 and other design codes generally ask for “realistic” nonlinear structural models. Higher degrees of realism usually imply more complex models. In the scope of the project ERIES-ALL4wALL (Almeida *et al.*, 2024) some of the currently most advanced simulation techniques for RC walls are being compared. They include some advanced and computationally heavy numerical approaches, such as detailed finite element simulations and applied element modelling, as well as other more computationally friendly methods, such as the multiple-vertical-line-element method and nonlinear beam-truss models (Hoult, Correia and Almeida, 2023). In the scope of the present technical session, “SDM-10: Seismic Nonlinear Modelling of Buildings in the Engineering Practice: Design and Assessment”, the present study will focus on the type of finite element (FE) that is considered to be on the forefront of engineering practice: beam (and/or truss) models with distributed plasticity through cross-sectional fibre discretization. They are widely available in many research-oriented and commercially available software and, to the knowledge of the authors, are widely used in practice. The simplest use of these elements considers individual beam-column models as a proxy for the entire wall (also known as line models), wherein the FE cross-section corresponds to the cross-section of the wall (Almeida, Tarquini and Beyer, 2016). Another more detailed discretization of the wall into vertical segments (e.g., the web and flanges of U-shaped walls) connected with horizontal links has given rise to the so-called wide-column models (Beyer, Dazio and Priestley, 2008a), but the definition of some input properties of these models is difficult. Finally, the most thoroughly discretised modelling of the wall – which will be adopted in the present study – gives rises to the so-called beam-truss models (BTMs) (Hoult, Correia and Almeida, 2023). They essentially consist of three-dimensional lattice models, which have also been used for the simulation of the experimental torsional and biaxial cyclic response of RC structural members (Miki and Niwa, 2004). This strategy has been further developed by Lu and Panagiotou (Lu and Panagiotou, 2012, 2014), who applied a 3D BTM model for nonplanar RC walls accounting for mesh-size effects. They use nonlinear beam and truss elements in the vertical and horizontal directions, nonlinear truss elements in the diagonals to represent the diagonal field of concrete, and linear elastic beams to simulate the out-of-plane stiffness.

2 Effective stiffness

2.1 Definitions

In the present work, the two following alternative definitions for effective stiffness K_{eff} proposed by Li and Xiang (2011) will be considered:

1. Method 1: The slope of the secant to the shear force vs lateral displacement curve crossing the point at 75% of the maximal shear force.
2. Method 2: The slope of the secant to the shear force vs lateral displacement curve at first yield. The latter is identified by the first tensile yield of longitudinal reinforcement, or by the cover concrete compression crushing strain of 0.002, whichever occurs at lower drifts.

The second definition ("Method 2") can (and will) be applied if strain demands in the outermost longitudinal reinforcement under highest tension, as well as in the compressed concrete cover, are available. Since this is rarely the case for experimental test results, it implies that such method is employed just for numerical model results.

The effective stiffness K_{eff} is often also described, alternatively, in terms of the effective moment of inertia I_{eff}. The latter is the one holding meaning for engineering practice, since it is the required input parameter for the definition of the members' cross-section in the model. More details on how the effective stiffness K_{eff} is transformed in I_{eff} is given in Section 6. Additionally, it is common to express K_{eff} and I_{eff} in terms of their gross counterparts, i.e. K_g and I_g, i.e. through an effective stiffness ratio K_{eff} / K_g, or I_{eff} / I_g.

2.2 Design code values and expressions for non-rectangular walls

Design codes propose different values for the effective stiffness. As mentioned above, the latter is usually described in terms of the effective moment of inertia I_{eff}, and sometimes dependent on the applied axial load ratio (ALR; the ratio of the applied axial load N by the load capacity of the element, $A_g f_c$, where A_g corresponds to the gross-sectional area of the wall and f_c to the concrete compressive strength) or on the cracked/uncracked condition of the element:

- The Eurocode 8 (CEN, 2004) indicates that, unless further analyses have been made on the cracked elements, the effective stiffness should be half of the uncracked stiffness, i.e. K_{eff} / K_g = I_{eff} / I_g = 0.5.
- The American Concrete Institute (ACI) proposes a value of 0.35 for cracked wall sections and 0.70 for uncracked stiffness (American Concrete Institute, 2008).
- FEMA (Federal Emergency Management Agency, 2000) follows a similar approach as the ACI and suggests the use of a value of 0.5 for previously cracked walls and 0.8 for uncracked walls.
- The 1994 Canadian concrete code (Canadian Portland Cement Association, 1995) suggested, for simplicity, a value of 0.7, regardless of the axial load ratio. This value is still widely used by Canadian designers. The 2014 edition of CSA (CSA Committee A23.3, 2004) proposes a new expression based on the ratio of the elastic bending moment demand to the actual flexural strength of the walls (Adebar and Dezhdar, 2015).
- The New Zealand concrete code recommends a value of 0.25 for walls without any axial load and 0.35 for walls with an axial load ratio of 10% (Adebar and Dezhdar, 2015).

A summary of several methods proposed for estimating the effective stiffness can be found in the work by Zhang and Li (2018). The same authors conclude their study by proposing modified methods for non-rectangular walls with different sectional shapes and loading directions, based on empirical expressions accounting for possible shear deformation contributions.

3 Beam-truss modelling and experimental database considered

3.1 Background considerations on beam-truss modelling

BTMs consists of an assembly of vertical, horizontal and diagonal elements. Each node constitutes a connection point between these elements, as shown in Figure 1.

Previous works suggest using the following equation to determine the angle of the diagonal elements with respect to the horizontal (Lu, Panagiotou and Koutromanos, 2016):

$$\theta_d = tan^{-1}\left(\frac{V_{max}}{f_{y,t}\rho_t t_w d}\right) \leq 65^{\circ} \qquad (1)$$

where V_{max} represents the maximal shear force. The latter can be obtained from the experimental force-displacement curve, if it is available (which is the case for the current work). The parameter ρ_t corresponds to the ratio of transverse reinforcement of yield strength $f_{y,t}$, t_w is the thickness of the wall, and d is the distance between the outer vertical elements in the loading direction.

The same document also recommends having an angle θ_d greater than 45º, showing that a too small angle can lead to underestimating the maximum lateral force by several tens of percent. The BTM appears to fit best experimental results by having a similar angle for every diagonal element, large enough and close to the value obtained by equation (1).

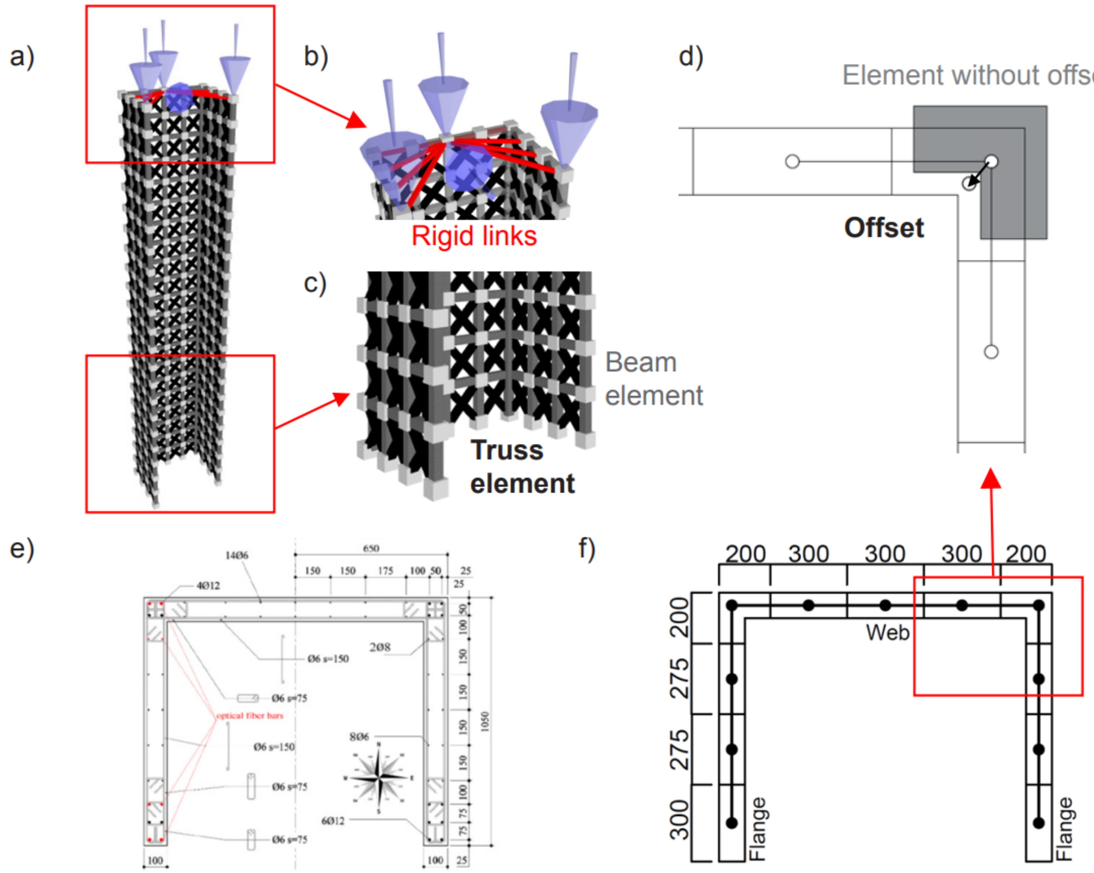

Figure 1. Illustration of a BTM approach for the U-shaped wall UW1: (a) View of the global model; (b) rigid links connecting the wall top nodes; (c) close-up of the vertical, horizontal, and diagonal elements; (d) offset definition for the corner elements; (e) cross-section reinforcement detailing, and (f) corresponding model discretisation [dimensions in mm].

3.2 Limitations in engineering practice

Practical engineering difficulties arise regarding the application of the angle given by equation (1). The first is that non-rectangular walls have, in general, different lateral force capacities in both directions since bending capacity is distinct, which provides distinct values for the diagonal angle θ_d. Since many of the BTM models will be in general used for pushover analyses in both directions, and/or dynamic analyses, a compromise needs to be reached.

Other additional factors constrain the discretization adopted in engineering practice, which are important to be mentioned. They include namely the limitations imposed by the combination of the length of each of the wall segments and the practical need to assign vertical elements at the wall boundary elements (if they exist) with a cross-sectional length corresponding to the length of the respective boundary element (since the latter corresponds to regions where confinement is usually assumed to be identical).

The wall models developed in the current manuscript reconcile, to the best of the authors' abilities, the above limitations.

3.3 Experimental database

A total of nine non-rectangular RC walls have been collected from the literature, covering various cross-sectional shapes (U-shaped, rectangular barbell-shaped, T-shaped and I-shaped) and loadings:

- UW1 is a large-scale U-shaped wall subjected to flexure, tested in the Institute of Mechanics, Materials and Civil Engineering (iMMC) at Université catholique de Louvain (UCLouvain), Belgium, in 2022 (Hoult, Doneux and Almeida, 2023). In Section 4.3 it is used as an illustrative example, for all the other walls presented in this study, regarding the simulation with BTM.

- TUA and TUB are two U-shaped walls studied and presented by Beyer, Dazio and Priestley (2008b).
- TUE, analysed by Hoult *et al.* (2020), is a slender U-shaped wall with a single layer of vertical reinforcement instead of the standard two layers.
- Unit 1.0 and Unit 2.0 are two barbell-shaped walls studied by Mestyanek (1986).
- TW2 and NTW1 are two T-shaped walls studied respectively by Thomsen IV and Wallace (1995) and (Brueggen, 2009).
- F1 is an I-shaped wall experimentally tested by Oesterle *et al.* (1976).

4 Simulation approach with application example for wall UW1

4.1 Simulation approach adopted

All numerical simulations are performed on *SeismoStruct*. A summary of the modelling options is presented next. An extensive study was performed with alternative combinations of finite element formulations for the vertical, horizontal, and diagonal elements, as well as different modelling proposals for the in-plane and out-of-plane response of the intersecting connections. Due to space limitations, the comparative results of all the models are not included. However, to put it simply, it was judged that the complexity of several of the explored options, together with specific challenging features of the associated model response, did not on average translate into an overall quality improvement in terms of numerical-experimental match. Therefore, and also in view of convenience of application in engineering practice, the retained modelling approach considered straightforwardly that all horizontal and vertical elements of the BTM were modelled by displacement-based finite element beams (*infrmDB* in *SeismoStruct*), whereas diagonals were simulated by truss elements. Nonlinear geometric effects were included.

Some of the vertical elements, namely in the boundary regions, contain longitudinal reinforcement and additional hoops in confined regions. Other vertical elements of the BTM do not require the assignment of transverse reinforcement as it is considered that confinement is negligible; this is also the case of the horizontal elements, whose “longitudinal” reinforcement is composed of the transverse rebars in the specific wall segment. In these cases (horizontal elements and vertical elements outside the confined BE regions), since *SeismoStruct* requires the definition of both longitudinal and transverse rebars in every section, a very low steel reinforcement ratio (with extremely large spacing) is defined for the transverse steel reinforcement; this implies the automatic computation of a confinement factor of 1. Truss (diagonal) elements have full concrete sections without reinforcement.

Regarding the material properties, they can be summed up as follows: (i) reinforcing bars are simulated with the Menegotto-Pinto model (Menegotto and Pinto, 1973); the fracture strain parameter is adjusted to 60% of the fracture strain reported from the available experimental monotonic tests (to account for buckling and cyclic low-cycle fatigue); (ii) concrete is simulated with the nonlinear model proposed by Mander, Priestley and Park (1988), assigning the compressive strength reported from available tests as the mean strength; wherever experimental tensile strength results are not available, its value was determined according to (CEN, 2004). As practiced by others, the tensile strength of the concrete in the diagonal elements was ignored (Arteta *et al.*, 2019) and no reinforcement is considered in its cross-section, as mentioned above. Unlike in other investigations (Murcia-Delso et al., 2024), the finite element formulations implemented in SeismoStruct do not yet allow to account for the effect of the diagonal normal tensile strain on the compressive resistance. The tensile strength in the horizontal elements was also ignored. Our numerical tests showed that accounting for the tensile strength in horizontal and diagonal elements tended to create numerical instability, manifested in the form of short peaks and troughs in the pushover response. In other words, tensile strength is only assigned to the vertical elements.

The wall models were subjected to both axial load and a time-history of static lateral displacements – some of the latter along the horizontal diagonal direction as well – according to the respective experimental programme. The reinforced concrete self-weight is assigned to the density of the reinforcement and the concrete of the BTM vertical elements, whereas the horizontal beams and diagonal trusses are considered weightless.

4.2 Limit states and performance criteria

During the analyses, various control points are defined to represent the following limit states related to the outermost cover and confined concrete fibres, and steel rebars (N.B.: compressive strains are negative):

1. Concrete crushing, $\varepsilon_{c,crushing} = -0.002$.
2. Steel rebar yield strain, ε_y, corresponding to the yield strain reported experimentally. The latter limit state is important to evaluate the effective stiffness of the wall, according to the second definition of effective stiffness as discussed in Section 2.1.
3. Steel rebar fracture strain, ε_{su}. As discussed above, the value corresponding to 60% of the fracture strain reported experimentally was assigned.
4. Ultimate compression strain for confined concrete, $\varepsilon_{cu,c} = -0.004 - \frac{1.4\rho_s f_{ym}\varepsilon_{su}}{f_{cm,c}}$, where ε_{su} refers to the confining reinforcement fracture strain, f_{ym} represents the confining rebar yield strength, ρ_s is calculated as the proportion of steel volume in the BTM vertical element representing the wall boundary element, and $f_{cm,c}$ is the confined compressive concrete strength (Priestley, Calvi and Kowalsky, 2007).

The above limit states were only applied to the vertical elements: whereas the first two are directly linked with the 2nd method for the definition of the effective stiffness, the last two relate to the definition of V_{max}. Such limit states leave out several other damage modes, including lap-splice slip, shear sliding, inclined (shear) cracks, etc. Rebar buckling and low-cycle fatigue are indirectly accounted for, in a simplistic way, by the application of the aforementioned factor of 60% to the steel rebar fracture strain. For a more extensive consideration of damage states associated with different performance levels, one can refer for instance to the recent work by Murcia-Delso *et al.* (2024).

4.3 Application example: wall unit UW1

This section illustrates in more detail the process to obtain the characteristics and properties of the BTM of wall unit UW1. This unit was tested experimentally by Hoult, Doneux and Almeida (2023). The geometry and detailing of the U-shaped cross-section is depicted in Figure 1 (e). The wall is modelled with a total height of 6720 mm – as observable in Figure 1 (a), corresponding to the shear span effectively applied during the test. The lateral displacement results presented hereinafter refer, however, to a height of 2250 mm, which corresponds to the height of the collar of the experimentally-tested unit. An axial load ratio (ALR) of 5% was also applied to the unit and corresponding model. The wall top nodes are connected through rigid links to a master node, as illustrated in Figure 1 (b), to which the incremental displacement is imposed; the slave nodes are restrained only along the two horizontal directions, i.e. in other words the rotation along the three axes, as well as vertical displacements, are not restrained. Such approach was used for all the wall units. The nodes at the base are assigned full fixity. Figure 1 (f) shows the discretization of the BTM vertical elements along the cross-section, whereas Figure 1 (a) shows the discretization along the height; as discussed in Section 3.2, the adopted discretization was a result of the following constraints: (i) length of the confined boundary element regions (i.e., flange ends and flange/web intersections); (ii) the angle suggested by equation (1), which provides a value of $\theta_d = 47.3°$; (iii) the need to monitor the lateral displacements at a height of approximately 2250 mm. Figure 1 (d) also illustrates the need to apply a diagonal offset to the corner vertical elements in the intersection between the web and the flange, to account for the fact that aligning the corresponding centre of gravity (CG) with the CG of the vertical elements along the web and the flanges would result in an incorrect positioning of such corner element. A complete description of the loading protocol and of the material properties of the wall can be found in Hoult, Correia and Almeida (2023), which also provides some results obtained with a similar BTM for the same test unit. Other parameters, including the strain limits, are reported in Saegerman, (2023). The pushover responses in the South-North and North-South directions – which will be used in Section 5 to compute the effective stiffness – can be seen in Figure 2, together with the experimental results and the indication of the limit strains.

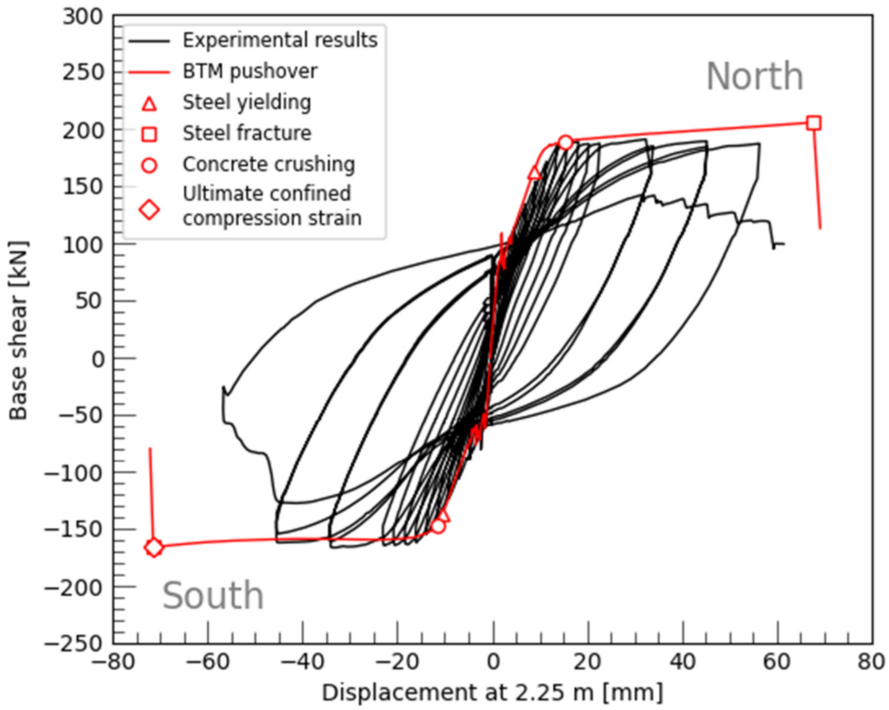

Figure 2. Comparison between the numerical pushover and the experimental cyclic results for Unit UW1, obtained with the BTM, with indication of the limit states.

5 Pushover *vs* experimental results for complete database

Figure 3 shows the pushover results obtained with BTM for all the remaining walls in the database indicated in Section 3.3, together with the experimental cyclic response. Due to space limitations, only the results obtained along the two main perpendicular directions of the wall units are presented. Future works will include results referring to the diagonal directions. The comparisons show that, despite the dispersion, overall the BTM provides a reasonable agreement with the envelope of the units' cyclic response, namely for the units with U-shaped and I-shaped cross sections. For one of the T-shaped walls (TW2) and the barbell-shaped ones, the match is less favourable. It is noted that, for all the numerical simulations except along the East-West (EW) direction of wall TW2, the first yield of longitudinal reinforcement was always attained for drifts smaller than those corresponding to cover concrete crushing.

6 Assessment of the effective moment of inertia

On the consideration that K_{eff} / K_g = I_{eff} / I_g, Figure 4 plots the values of the effective moment-of-inertia ratios for the set of wall units, as simulated with BTMs, according to the two definitions or methods introduced in Section 2.1. The ratios are expressed in relation to the gross moment of inertia of each wall along the same direction. For the application of Method 1 to compute the effective stiffness, V_{max} is determined based on the first reaching of the steel rebar fracture strain ε_{su} or the ultimate compression strain for confined concrete $\varepsilon_{cu,c}$, along the direction in consideration. Figure 4 also plots the values of the effective stiffness computed from the experimental results (with black circle markers), using Method 1; Method 2 cannot be applied since the first yield point is not identified in most experiments). The maximum experimental shear force V_{max} along the direction under analysis is considered. The vertical lines represent the values of effective stiffness ratios recommended by the design codes as indicated in Section 2.2.

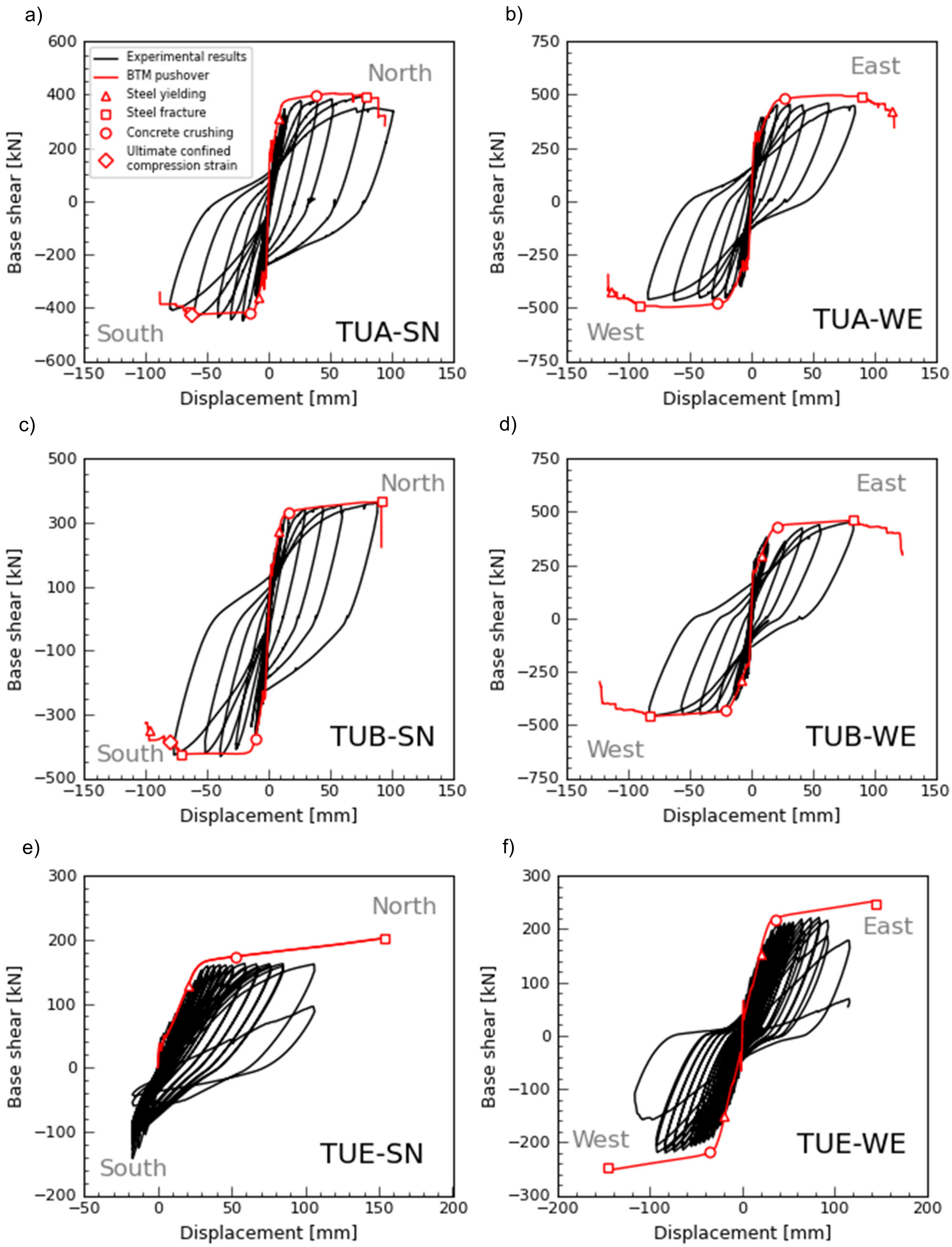
a)
Experimental results
BTM pushover
Steel yielding
Steel fracture
Concrete crushing
Ultimate confined compression strain
North
South
TUA-SN
Base shear [kN]
Displacement [mm]
b)
East
West
TUA-WE
Base shear [kN]
Displacement [mm]
c)
North
South
TUB-SN
Base shear [kN]
Displacement [mm]
d)
East
West
TUB-WE
Base shear [kN]
Displacement [mm]
e)
North
South
TUE-SN
Base shear [kN]
Displacement [mm]
f)
East
West
TUE-WE
Base shear [kN]
Displacement [mm]

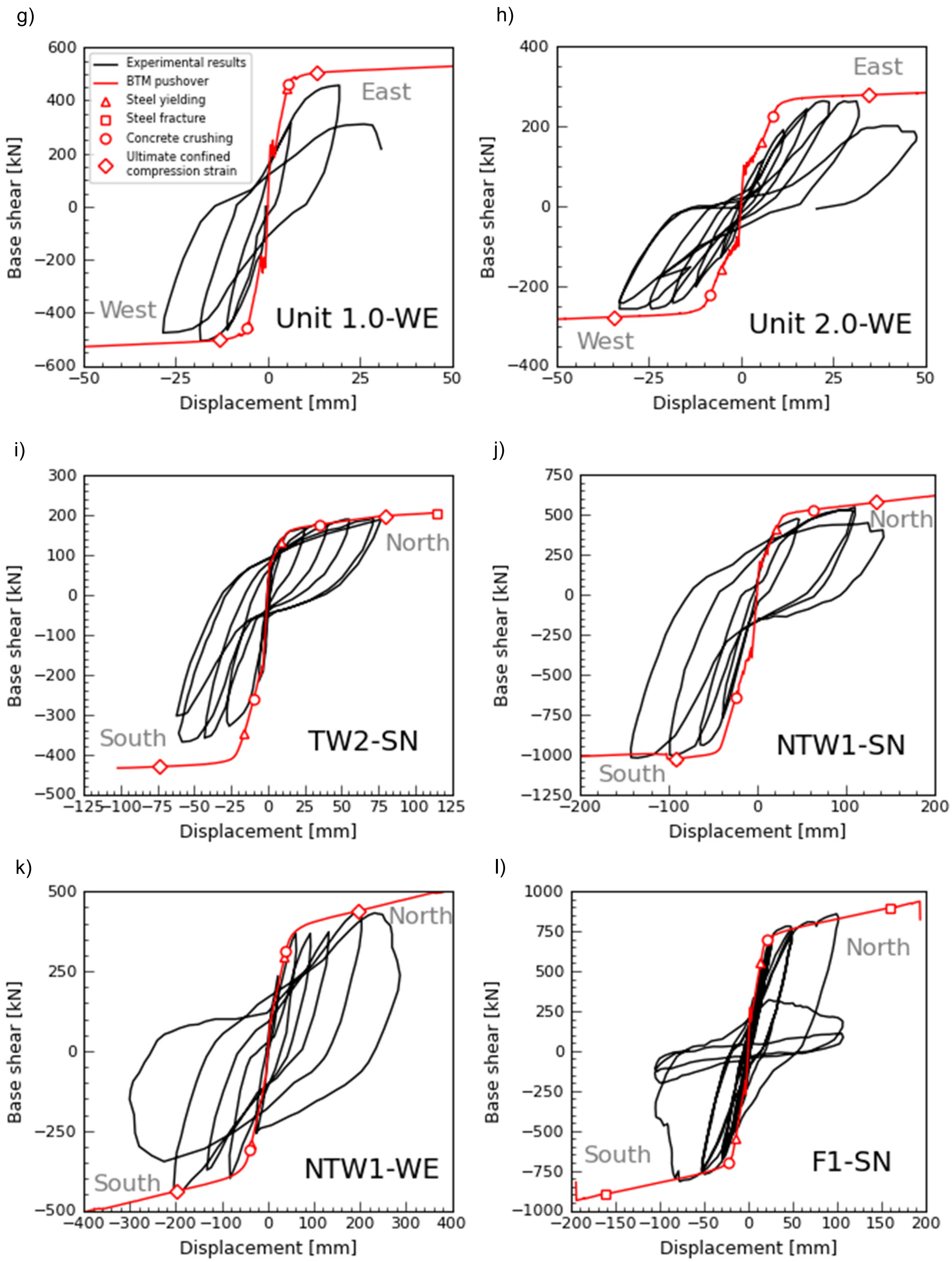

Figure 3. Pushover results for unit: (a) TUA, South-North; (b) TUA, West-East; (c) TUB, South-North; (d) TUB, West-East; (e) TUE, South-North; (f) TUE, West-East; (g) Unit 1.0, West-East; (h) Unit 2.0, West-East; (i) TW2, South-North; (j) NTW1, South-North; (k) NTW1, West-East; (l) F1, South-North.

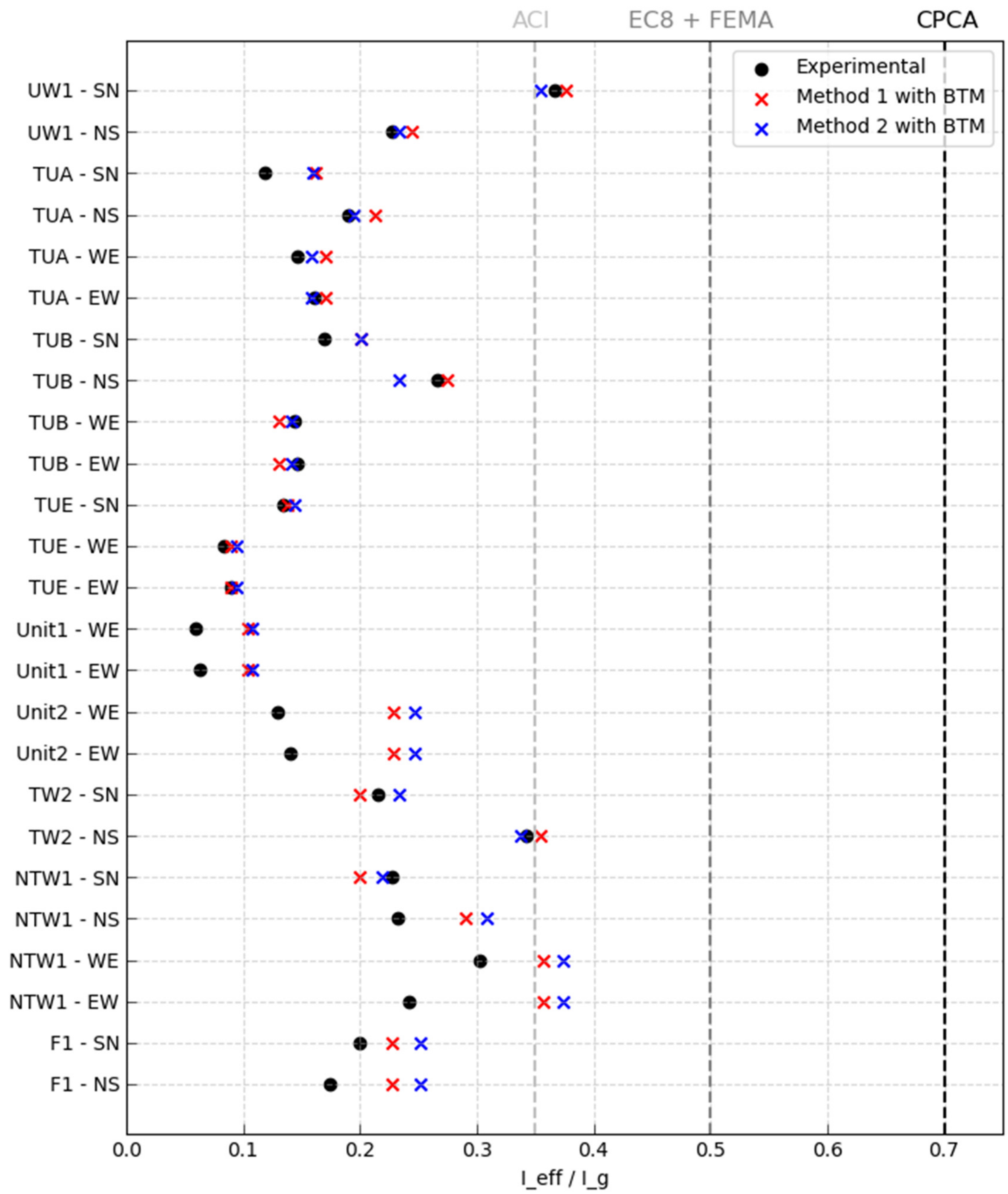

Figure 4. Comparison of the effective moment of inertia ratios for the non-rectangular wall database, as computed from: (i) experimental data; (ii) beam-truss models; (iii) design code expressions.

Some brief conclusions can be gathered: (i) the experimental effective stiffness ratio for the analysed walls varies roughly between 6% and 37.5%, which is a considerable range; (ii) apart from some units and directions, the match between the effective stiffness ratios computed from the BTM models and the experimental tests is satisfactory, which points to promising applications in engineering practice; (iii) in general, methods 1 and 2 provide similar results; (iv) code expressions tend to overestimate the effective stiffness ratios.

7 Conclusions

In the past decade, there has been an exponential enhancement in the seismic nonlinear analysis capabilities of software packages. Their utilisation has expanded beyond the realm of research, gaining prevalence in the professional community. The technical session to which the present paper is addressed aims to foster a dialogue on the practical applications of nonlinear analysis in real-world scenarios, delving into the current feasibility, existing challenges, and future directions in this domain. With such background in mind, the current work explored the coupling of an important engineering parameter – the effective stiffness of reinforced concrete walls, which critically impact force-based (FB) design and assessment of buildings – with the application of a state-of-the-practice engineering model – the nonlinear beam-truss model (BTM). Recent studies have shown that an unsatisfactory determination of the effective stiffness of vertical members is at the heart of significant discrepancies between FB and displacement-based (DB) methods of seismic design and analysis. The study focuses on non-rectangular walls, thus covering an important gap in the literature since existing studies address almost exclusively rectangular sections; which contrasts the fact that most building core walls are non-rectangular. In practice, this study assembled a database of experimental cyclic tests on non-rectangular walls (U-shaped, barbell-shaped, T-shaped, and F-shaped) and determined, from those tests, the corresponding effective stiffnesses. It went on to perform pushover analyses of these same walls with BTMs, which is a numerical modelling technique still seldom used in engineering practice. Finally, the determination of the corresponding effective stiffnesses from the abovementioned results was also performed, as well as a final comparison with recommendations from codes.

The following conclusions can be extracted: (i) in general, the BTMs provided a reasonable agreement with the envelope of the units' cyclic response; additionally, the computational time was small for pushover analyses and can therefore be considered a desirable practical tool for nonlinear static analyses of RC buildings and DB design and assessment; (ii) BTMs also proved their ability to determine the effective stiffness of walls, outputting overall similar results to those obtained experimentally; (iii) the reduction factors for the effective stiffness proposed by current design codes are not applicable to non-rectangular walls, providing a clear overestimation with implications on artificially large seismic design demands, incompatible with more accurate DB approaches; (iv) the use of BTM models, applied to a further extended variety of cross-sectional shapes (e.g., E- shaped and L-shaped), can be used to derive more applicable design expressions.

It is hoped that this study contributes to transfer the use of nonlinear BTMs from research to practical applications in engineering, in which they can now be readily accommodated both in terms of computational capacity and from the technical viewpoint. Further, in view of its importance for seismic design, it is the authors' wish that it spurs the development of more accurate expressions for the effective moment-of-inertia of non-rectangular cross sections, and the corresponding adoption by international design and assessment codes.

8 References

Adebar, P. and Dezhdar, E. (2015) 'Effective stiffness for linear dynamic analysis of concrete shear wall buildings: CSA A23.3-2014', in *11th Canadian Conference on Earthquake Engineering*, pp. 1–8.

Almeida, J. P. *et al.* (2024) 'Shake-table testing of two u-shaped RC walls : Overview of the project ERIES-ALL4wALL', in *18th World Conference of Earthquake Engineering (WCEE2024)*.

Almeida, J. P. de *et al.* (2022) 'Harmonising force-based and displacement-based design approaches for the next generation of Eurocode 8: Application to reinforced concrete moment resisting frames', *Engineering Structures*, 272.

Almeida, J. P., Tarquini, D. and Beyer, K. (2016) 'Modelling Approaches for Inelastic Behaviour of RC Walls: Multi-level Assessment and Dependability of Results', *Archives of Computational Methods in Engineering*, 23(1), pp. 69–100. doi: 10.1007/s11831-014-9131-y.

American Concrete Institute (2008) *ACI 318-08: Building code requirements for structural concrete and commentary*.

Arteta, C. A. *et al.* (2019) 'Hybrid approach for simulating shear–flexure interaction in RC walls with nonlinear truss and fiber models', *Bulletin of Earthquake Engineering*, 17(12), pp. 6437–6462. doi: 10.1007/s10518-019-00681-6.

Beyer, K., Dazio, A. and Priestley, M. J. N. (2008a) 'Inelastic wide-column models for U-shaped reinforced concrete walls', *Journal of Earthquake Engineering*, 12(SUPPL. 1), pp. 1–33. doi: 10.1080/13632460801922571.

Beyer, K., Dazio, A. and Priestley, M. J. N. (2008b) 'Quasi-static cyclic tests of two U-shaped reinforced concrete walls', *Journal of Earthquake Engineering*, 12(7), pp. 1023–1053. doi: 10.1080/13632460802003272.

Brueggen, B. L. (2009) 'Performance of T-shaped reinforced concrete structural walls under multi-directional loading', *PhD Thesis, University of Minnesota*.

Canadian Portland Cement Association (1995) *"Explanatory notes on CSA Standard A23.3-94," Part 1, Concrete Design Handbook*.

CEN (European Committee for Standardization) (2004) *Eurocode 8 — Design of structures for earthquake* *resistance - Part 1: General rules, seismic actions and rules for buildings*.

CEN (European Committee for Standardization) (2022) *Eurocode 8 — Design of structures for earthquake resistance — Part 1-1: General rules and seismic action (Working Draft)*.

CSA Committee A23.3 (2004) *“Design of Concrete Structures: Structures (Design) – A National Standard of Canada” Canadian Standards Association*.

Federal Emergency Management Agency (2000) *FEMA 356 Prestandard and Commentary for the Seismic Rehabilitation of Buildings, ASCE*.

Hoult, R. *et al.* (2020) ‘Seismic performance of slender RC U-shaped walls with a single-layer of reinforcement’, *Engineering Structures*, 225. doi: 10.1016/j.engstruct.2020.111257.

Hoult, R., Correia, A. A. and Almeida, J. P. (2023) ‘Beam-truss models to simulate the axial-flexural-torsional performance of RC U-Shaped wall buildings’, *CivilEng*, 4(1), pp. 292–310. doi: 10.3390/civileng4010017.

Hoult, R., Doneux, C. and Almeida, J. P. (2023) ‘Tests on reinforced concrete U-shaped walls subjected to torsion and flexure’, *Earthquake Spectra*, pp. 1–26. doi: 10.1177/87552930231195315.

Kolozvari, K. *et al.* (2018) ‘Comparative study of state-of-the-art macroscopic models for planar reinforced concrete walls’, *ACI Structural Journal*, 115(6), pp. 1637–1657. doi: 10.14359/51710835.

Li, B. and Xiang, W. (2011) ‘Effective Stiffness of Squat Structural Walls’, *Journal of Structural Engineering*, 137(12), pp. 1470–1479. doi: 10.1061/(asce)st.1943-541x.0000386.

Lu, Y. and Panagiotou, M. (2012) *Three-Dimensional Nonlinear Cyclic Beam-Truss Model for Non-Planar Reinforced Concrete Walls*.

Lu, Y. and Panagiotou, M. (2014) ‘Three-Dimensional Cyclic Beam-Truss Model for Nonplanar Reinforced Concrete Walls’, *Journal of Structural Engineering*, 140(3), p. 04013071. doi: 10.1061/(asce)st.1943-541x.0000852.

Lu, Y., Panagiotou, M. and Koutromanos, I. (2016) ‘Three-dimensional beam-truss model for reinforced concrete walls and slabs – part 1: modeling approach, validation, and parametric study for individual reinforced concrete walls’, *Earthquake Engineering and Structural Dynamicsg*, 45(9), pp. 1495–1513. doi: 10.1002/eqe.2719.

Mander, J. B., Priestley, M. J. N. and Park, R. (1988) ‘Theoretical stress-strain model for confined concrete’, *Journal of Structural Engineering*, 114(8), pp. 1804–1825.

Menegotto, M. and Pinto, P. (1973) ‘Method of analysis for cyclically loaded R.C. plane frames including changes in geometry and non-elastic behavior of elements under combined normal force and bending’, in *Proc. of the Symposium Resistance and Ultimate Deformability of Structures Loads, Acted on by Well-Defined Repeated*. Lisbon, Portugal.

Mestyanek, J. M. (1986) *The earthquake resistance of reinforced concrete structural walls of limited ductility*. University of Christchurch, New Zealand.

Miki, T. and Niwa, J. (2004) ‘Nonlinear analysis of RC structural members using 3D lattice model’, *Journal of Advanced Concrete Technology*, 2(3), pp. 343–358. doi: 10.3151/jact.2.343.

Murcia-Delso, J. *et al.* (2024) ‘New framework for seismic evaluation of RC wall structures based on simulation and material strains’, in *18th World Conference of Earthquake Engineering (WCEE2024)*.

Oesterle, R. G. *et al.* (1976) ‘Earthquake resistant structural walls - Tests of isolated walls’, *Research and Development Construction Technology Laboratories, Portland Cement Association*.

Priestley, M. J. N., Calvi, G. M. and Kowalsky, M. J. (2007) *Displacement-based Seismic Design of Structures*. IUSS Press - Istituto Universitario di Studi Superiori di Pavia.

Saegerman, C. (2023) ‘Influence of axial load ratio and eccentricity on the cyclic response of non-rectangular walls through beam-truss models’, *MSc Thesis, Université catholique de Louvain*.

Samanta, N. and Dasgupta, K. (2024) ‘Improving the seismic behaviour of flanged slender RC structural wall using enlarged boundary element’, in *18th World Conference of Earthquake Engineering (WCEE2024)*.

Thomsen IV, J. H. and Wallace, J. W. (1995) ‘Displacement—Based Design of Reinforced Concrete Structural Walls: An Experimental Investigation of Walls with Rectangular and T-Shaped Cross-Sections’, *Nsf*, pp. 1–375. Available at: http://nisee.berkeley.edu/elibrary/Text/200606122.

Vuran, E. *et al.* (2024) ‘Damage observations of RC buildings from 2023 Kahramanmaraş earthquake sequence and discussion on the seismic code regulations’, *Bulletin of Earthquake Engineering*, (February 2023). doi: 10.1007/s10518-023-01843-3.

Zhang, Z. and Li, B. (2018) ‘Effective Stiffness of Non-Rectangular Reinforced Concrete Structural Walls’, *Journal of Earthquake Engineering*, 22(3), pp. 382–403. doi: 10.1080/13632469.2016.1224744.